

Interface dynamics of wet active systems

Fernando Caballero,¹ Ananyo Maitra,^{2,3} and Cesare Nardini^{4,5}

¹*Department of Physics, Brandeis University, Waltham, MA 02453, USA**

²*Laboratoire de Physique Théorique et Modélisation, CNRS UMR 8089,*

CY Cergy Paris Université, F-95032 Cergy-Pontoise Cedex, France

³*Laboratoire Jean Perrin, UMR 8237 CNRS, Sorbonne Université, 75005 Paris, France*

⁴*Service de Physique de l'Etat Condensé, CEA, CNRS Université Paris-Saclay, CEA-Saclay, 91191 Gif-sur-Yvette, France*

⁵*Sorbonne Université, CNRS, Laboratoire de Physique Théorique de la Matière Condensée, LPTMC, F-75005 Paris, France*
(Dated: September 12, 2024)

We study the roughening of interfaces in phase-separated active suspensions on substrates. At large length and timescales, we show that the interfacial dynamics belongs to the $|\mathbf{q}|$ KPZ universality class discussed in Besse et al. Phys. Rev. Lett. **130**, 187102 (2023). This holds despite the presence of long-ranged fluid flows. At early times, instead, the roughening exponents are the same as those in the presence of a momentum-conserving fluid. Surprisingly, when the effect of substrate friction can be ignored, the interface becomes random beyond a de Gennes-Taupin lengthscale which depends on the interfacial tension.

The scale-free, or rough, properties of interfaces is a well-studied problem in statistical mechanics [1, 2]. Early theoretical investigations [3–5] centred on the Eden model [6], originally proposed to describe the shape of cell colonies, and the ballistic deposition model [7]. The Kardar-Parisi-Zhang (KPZ) universality class [8, 9] was a major breakthrough, unifying under its universality class a large set of different processes [10]. However, a large class of interfaces—those with a conserved average height—cannot be described by the KPZ equation [1, 11, 12].

Examples of interfaces not belonging to the KPZ universality class are found in phase-separated systems. Already in equilibrium systems, since diffusive or fluid fluxes in the bulk relax much faster than the low wavenumber fluctuations of the interface itself, the interfacial dynamics becomes nonlocal and, even at linear level, does not obey Edwards-Wilkinson scaling [13, 14]. Specifically, a small amplitude height fluctuation $h_{\mathbf{q}}$ on wavevector \mathbf{q} over a flat d -dimensional plane obeys

$$\partial_t h_{\mathbf{q}}(t) = -\gamma|\mathbf{q}|^a h_{\mathbf{q}}(t) + \sqrt{2D|\mathbf{q}|^{-2+a}}\xi_{\mathbf{q}}, \quad (1)$$

where $\xi_{\mathbf{q}}$ is a Gaussian white noise, and γ is proportional to interfacial tension. When the underlying dynamics of the density field is diffusive, $a = 3$; $a = 1$ for systems dominated by hydrodynamic effects. Importantly, in either case, the structure factor of the interface depends on wavenumber as $S(\mathbf{q}) = \langle |h_{\mathbf{q}}|^2 \rangle \sim |\mathbf{q}|^{-2}$, which is commonly referred to as capillary wave theory [15]. In equilibrium systems, Eq. (1) is believed to be exact for the large-scale properties in the steady state because there are no additional terms that are relevant in the renormalization group (RG) sense. Hence, the scale-free properties of the interface, commonly encoded in the roughening exponent χ and dynamical exponent z that determine the long-range behaviour of spatial and temporal correlations $\langle h(\mathbf{x}, t)h(\mathbf{x}', t) \rangle \sim |\mathbf{x} - \mathbf{x}'|^{2\chi}$ and $\langle h(\mathbf{x}, t)h(\mathbf{x}, t') \rangle \sim |t - t'|^{2\chi/z}$, are given by the linear the-

ory ($z = a$, $\chi = (2-d)/2$). Analogous linear descriptions of the interface have been recently obtained for active systems in the dry [16] and wet settings [17, 18]. However, in the presence of activity, a relevant non-linearity can singularly modify the dynamics of capillary waves and a new universality class, termed $|\mathbf{q}|$ KPZ, emerges in the absence of any fluid flow [19].

A primary reason for developing active matter theories is to bring mechanobiology within the ambit of condensed matter physics, and the vast majority of micro-biological systems require a fluid medium [20, 21]. Indeed, most experimentally studied active systems, both of biological and synthetic origin, are wet to some extent [22–28]. In most of these, active particles move in quasi-two-dimensional geometries, and the fluid flow is screened; one might thus conclude that the dry limit applies. It is however known that, even in the presence of screening, the fluid flows generated by active forces are long-ranged, decaying algebraically as $1/r^3$ [29], where r is the distance between the point at which the force is applied and the one where the flow is observed. Hence, even in the presence of substrate friction, and at sufficiently large scales, it is unclear whether the fully dry physics is recovered. This does not happen in other circumstances, such as for polar flocks: fluid flows, even when screened, have profound effects, for instance, eliminating [30–33] or modifying [34] giant number fluctuations.

In this Letter, we examine the physics of interfaces in active, isotropic suspensions in the presence of fluid flows. Our setup applies to active suspensions either on a substrate or in confined geometries, thus encompassing most experimentally studied realisations of active systems. At sufficiently large scales, we show that these interfaces belong to the $|\mathbf{q}|$ KPZ universality class and that the amplitude of the active force can be used as a control parameter to tune the strength of the $|\mathbf{q}|$ KPZ non-linearity. Intriguingly, in wavenumber regimes in which the fluid dynamics is not screened, the interface normals

become uncorrelated over large scales, and the growth does not follow a power law in time unlike in standard roughening scenarios; in this regime, the stationary structure factor becomes $S(\mathbf{q}) \sim |\mathbf{q}|^{-3}$, also at odds with the standard capillary-wave theory. Finally, for the specific case in which momentum is exactly conserved and hence the suspension is globally force-free, our results suggest that the interface dynamics remains linear.

We now show how we obtain these results. Our starting point is the natural description of the density field $\phi(\mathbf{r}, t)$ driven by advective and diffusive dynamics:

$$\partial_t \phi(\mathbf{r}, t) + \mathbf{v} \cdot \nabla \phi(\mathbf{r}, t) = M \nabla^2 \mu + \sqrt{2MD} \nabla \cdot \mathbf{\Lambda}_n, \quad (2)$$

where M is the mobility, $\mathbf{\Lambda}_n$ is a zero-average uncorrelated noise vector with unitary variance, \mathbf{v} is the incompressible velocity field ($\nabla \cdot \mathbf{v} = 0$), and $\mu = \delta F / \delta \phi$ is the chemical potential associated with the free energy F . The latter is a Landau-Ginzburg expansion of the phase field and its gradients $F = \int d\mathbf{r} \left[f(\phi) + (k/2)(\nabla \phi)^2 \right]$, where the bulk free energy density $f(\phi)$ is a double well. The flow field \mathbf{v} obeys

$$0 = \eta \nabla^2 \mathbf{v} - \Gamma \mathbf{v} - \nabla P + \mathbf{f} + \mathbf{f}^n, \quad (3)$$

in the low-Reynolds regime, where η is the viscosity, P is a pressure determined by incompressibility, \mathbf{f} is the total deterministic force density arising from density modulations. The noise term \mathbf{f}^n has zero average and a variance which, written in Fourier space, reads

$$\begin{aligned} \langle f_i^n(\mathbf{p}, \omega) f_j^n(\mathbf{p}', \omega') \rangle = \\ (2\pi)^{d+2} 2D(\Gamma + \eta|\mathbf{p}|^2) \delta_{ij} \delta(\mathbf{p} + \mathbf{p}') \delta(\omega + \omega'), \end{aligned} \quad (4)$$

where $\mathbf{p} = (\mathbf{q}, q_y)$ is the wave-vector in $d+1$ dimensional space and i denotes the spatial components. For simplicity, we assume that \mathbf{f}^n obeys a fluctuation-dissipation relation even in our active system.

Upon setting $\mathbf{f} = \mathbf{f}^p = -\phi \nabla \mu$ and $\Gamma = 0$, Eqs. (2) and (3) reduce to model H, the standard description of phase-separation in momentum-conserved systems [35, 36]. Notice that $\Gamma \neq 0$ implies that momentum is not conserved. This naturally arises in two cases: either due to friction of the active fluid with the substrate or, even when this is strictly absent, if the fluid is confined vertically by no-slip walls [29, 37]. In the latter case, once the vertical motion is averaged out, the ensuing effective two-dimensional description leads to Eq. (3), and the screening length $1/\lambda = \sqrt{\eta/\Gamma}$ turns out to be proportional to the film thickness [29, 30, 33, 37, 38]. With a slight abuse of terminology, we will keep referring to Γ as the friction in either case. It is crucial for the following that, despite screening, the fluid flow disturbances still decay algebraically for $r \gg 1/\lambda$: friction only renormalises the decay from a $1/r^2$ scaling in unbounded suspensions to a $1/r^3$ in the present case [29], implying that the suspension still interacts non-locally.

We now describe how to introduce activity in Eqs. (2) and (3). As in previous attempts at describing wet active suspensions [35, 39], activity breaks the relation between \mathbf{f} and the gradients of the chemical potential so that $\mathbf{f} = \mathbf{f}^p + \mathbf{f}^a$. If momentum is conserved, the force density must come from a stress tensor σ_{ij} , with $f_i^a = \nabla_j \sigma_{ij}$. Expanding the stress tensor to leading order in gradients yields $\sigma_{ij} = \kappa(\nabla_i \phi \nabla_j \phi - \delta_{ij} |\nabla \phi|^2 / (d+1))$, a model known as the Active Model H [39]. When $\Gamma \neq 0$, active forces that cannot be written as the divergence of a local stress tensor are also present. In this case, including all terms up to order $\mathcal{O}(\nabla^3 \phi^3)$ in \mathbf{f}^a , we find

$$f_i^a = K_1 \phi (\nabla^2 \phi) \nabla_i \phi + K_2 |\nabla \phi|^2 \nabla_i \phi. \quad (6)$$

A distinct natural way to introduce activity is to use a force density that pushes the interface in the direction normal to it (this is particularly natural if the interface is a membrane hosting active inclusions [40–42]). Denoting by $h(\mathbf{x})$ the height of the interface, this corresponds to

$$\mathbf{f}^a = 2\alpha_f \hat{\mathbf{n}} \delta(y - h), \quad (7)$$

where $\hat{\mathbf{n}} = (\hat{y} - \hat{x} \nabla h) / \sqrt{1 + (\nabla h)^2}$ is the interface normal. This force density is such that its strength is proportional to α_f , and points from the dense to the dilute regions [43]. We will show that introducing activity either via Eq. (6) or Eq. (7) leads to the same results, hence showing that our conclusions are generically valid.

In the case of model H, the interface height is described by Eq. (1) with $a = 1$ [13, 14]. This can be shown by neglecting diffusive fluxes (i.e. setting $M = 0$ in Eq. (2)), which contribute at higher order in gradients, and assuming that the density profile φ across the interface evolves quasistatically with respect to fluctuations of the interfacial height. The latter is equivalent to the ansatz, exact at leading order in h and $|\mathbf{q}|$, and in the absence of overhangs [13],

$$\phi(\mathbf{x}, y, t) = \varphi(y - h(\mathbf{x}, t)).$$

We now use the same technique to investigate the effect of the active forces and friction. We formally solve Eq. (3) with $M = 0$ to yield the following ϕ dynamics in closed form:

$$\partial_t \phi(\mathbf{r}, t) = -\partial_i \phi(\mathbf{r}, t) \int d\mathbf{r}' T_{ij}(\mathbf{r} - \mathbf{r}') f_j(\mathbf{r}') + \tilde{\xi}(\mathbf{r}), \quad (8)$$

where the Gaussian noise $\tilde{\xi}$ has zero average and the variance

$$\langle \tilde{\xi}(\mathbf{r}, t) \tilde{\xi}(\mathbf{r}', t') \rangle = 2D \partial_i \phi(\mathbf{r}) T_{ij}(\mathbf{r} - \mathbf{r}') \partial_j \phi(\mathbf{r}') \delta(t - t'). \quad (9)$$

Here, T_{ij} are the components of a modified Oseen tensor, which are most conveniently written in Fourier space as

$$\tilde{T}_{ij}(\mathbf{p}) = \frac{1}{\Gamma + \eta|\mathbf{p}|^2} \left(\delta_{ij} - \frac{\mathbf{p}_i \mathbf{p}_j}{|\mathbf{p}|^2} \right). \quad (10)$$

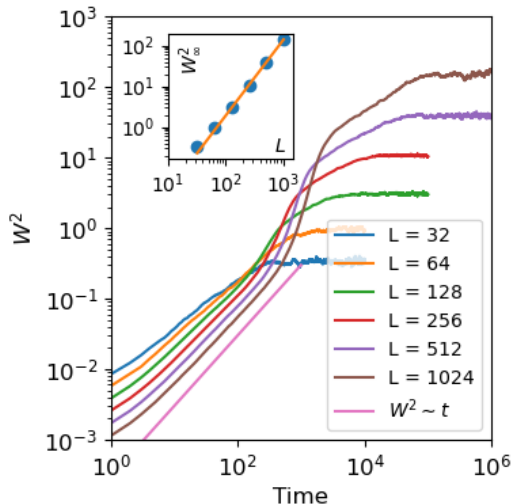


FIG. 1. Interface width W^2 as a function of time as obtained from numerical integration of Eq. (12) for screening length $1/\lambda = 1$ and $\bar{\alpha} = 0.63$. The inset shows the saturation values W_∞^2 as a function of system size L , with a power law fit with slope 1.85.

The only component of the Oseen tensor relevant to our treatment below is T_{yy} : the contributions to Eq. (8) from all other components either vanish, turn out to be irrelevant in the RG sense, or can be reabsorbed in pressure jumps across the interface. It is useful to write T_{yy} in real space in y and Fourier space in \mathbf{x} , which we denote as $\mathcal{T}_{yy}(\mathbf{q}, y)$:

$$\mathcal{T}_{yy}(\mathbf{q}, y) = \frac{|\mathbf{q}|e^{-|\mathbf{q}||y|}}{2\eta\lambda^2} - \frac{|\mathbf{q}|^2 e^{-|y|\sqrt{\lambda^2+|\mathbf{q}|^2}}}{2\eta\lambda^2\sqrt{\lambda^2+|\mathbf{q}|^2}}. \quad (11)$$

Substituting Eq. (7) in Eq. (8), and expanding to lowest nonlinear order in h , we obtain the main analytical result of this Letter [44]:

$$\partial_t h_{\mathbf{q}} = -\gamma|\mathbf{q}|^2 \mathcal{T}_{yy}(\mathbf{q}, 0) h_{\mathbf{q}} + \alpha \mathcal{T}_{yy}(\mathbf{q}, 0) \mathcal{F}[(\nabla h)^2] + \xi_{\mathbf{q}} \quad (12)$$

where \mathcal{F} is the Fourier transform operator, and the Gaussian noise has zero average and correlations

$$\langle \xi_{\mathbf{q}}(t) \xi_{\mathbf{q}'}(t') \rangle = 2D(2\pi)^d \mathcal{T}_{yy}(\mathbf{q}, 0) \delta_{\mathbf{q}, -\mathbf{q}'} \delta(t - t'). \quad (13)$$

The nonlinear term proportional to α closely resembles the KPZ non-linearity but, crucially, comes with a \mathbf{q} -dependent prefactor encoded in the Oseen tensor. When the active force density is given by Eq. (7), we find $\alpha = \alpha_f$ [44]. When the activity given by Eq. (6), we show that $\alpha = (K_1 - 2K_2) \int du \varphi(u) \varphi'(u) \varphi''(u)$, where the integral is taken across the interface. In both cases, the amplitude of the leading non-linear term in Eq. (12) is directly proportional to the strength of the active force densities acting on the fluid. In Eq. (12) we have neglected nonlinearities that are higher order in h and are thus irrelevant in the RG sense.

We first investigate Eq. (12) numerically for one-dimensional interfaces ($d = 1$) using the package recently developed in [45]. This is a pseudo-spectral scheme with a computational complexity proportional to $N \log N$, where N is the number of collocation points, despite the non-local nature of Eq. (12). We monitor the interface width $W^2 = L^{-1} \int_0^L dx' (h - \bar{h})^2$, where \bar{h} is the average of $h(x, t)$ across the system. We then measure the scaling exponents χ and z using the fact that $W^2 \sim t^{2\chi/z}$ and that, once the interface width has saturated in time to its stationary value, $W_\infty^2 \sim L^{2\chi}$. These measures are standard in studies of roughening phenomena.

We integrate Eq. (12) for several system sizes, and average the results over multiple noise realizations (from 10^2 to 10^3 depending on system size). When $\alpha = 0$, our numerical measures yield the growth predicted by dimensional analysis, which corresponds to $z = 1$ and $\chi = 1/2$ [44]. We then performed simulations with $\bar{\alpha} \sim \mathcal{O}(1)$, where $\bar{\alpha} = \alpha \sqrt{D/\gamma^3}$ is the non-dimensional coupling setting the strength of the nonlinearity. Fig. 1 shows the width as a function of time and various system sizes for $\bar{\alpha} = 0.63$ and screening length $1/\lambda = 1$. At early times and large enough system sizes, we find $z \simeq 1$, which is the expected value for momentum conserving fluids [2, 14]; a linear theory suffices to obtain this result. The nonlinearity then kicks in and creates a regime of rapid growth, showing a clear deviation from classical roughening. For large system sizes ($L \geq 512$) and late times, W^2 seems to enter a second power-law regime before saturating, but we were unable to obtain a clear measure of the associated exponent up to system sizes that are computationally accessible. Finally, the width saturates to a value that depends on L , as expected in a standard roughening scenario. The associated measure for χ is shown in the inset of Fig. 1 and is compatible with $2\chi \simeq 1.85$, greater than the value expected from the linear theory ($2\chi = 1$).

An accurate numerical study of Eq. (12) showing the scaling at both early and late times for a single set of parameters is computationally prohibitive. Therefore, to gain insight into the various regimes, we consider different limits of Eq. (12) and investigate them both analytically and numerically. First, we show that friction is dominant at late enough times and low enough wavenumbers $|\mathbf{q}|$. Indeed, for $|\mathbf{q}| \ll \lambda$, one can show that

$$\mathcal{T}_{yy}(\mathbf{q}, 0) \rightarrow_{|\mathbf{q}| \ll \lambda} \frac{|\mathbf{q}|}{2\eta\lambda^2} \quad (14)$$

and hence Eq. (12) becomes

$$\partial_t h_{\mathbf{q}}(t) = -\frac{\gamma|\mathbf{q}|^3}{2\Gamma} h_{\mathbf{q}}(t) + \frac{\alpha|\mathbf{q}|}{2\Gamma} \mathcal{F}[(\nabla h(x, t))^2] + \xi_{\mathbf{q}}. \quad (15)$$

Eq. (15) is the $|\mathbf{q}|$ KPZ equation, first introduced in [19]. This result is remarkable and merits further comments. First, while it is expected that capillary waves relax on a

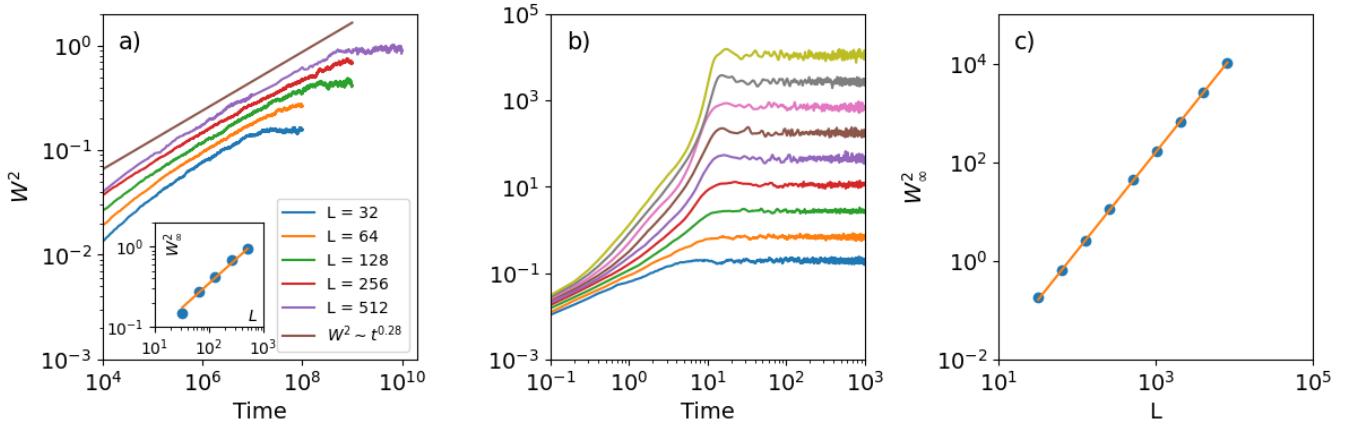


FIG. 2. Evolution of the width in two limits; a) In the fully screened limit, with $\bar{\alpha} = 0.6$, $\lambda = 10^3$ and sufficiently large system-size, we observe a growth law compatible with the $|\mathbf{q}|$ KPZ universality class ($W^2 \sim t^{0.28}$). The inset shows the saturation values W_∞^2 as a function of system size L , and a fit to a power law gives a slope of 0.61 ± 0.04 , compatible with the $|\mathbf{q}|$ KPZ universality class. b) In the unscreened limit, with $\lambda = 0$ (other parameters as in panel a), each line from bottom to top corresponds to systems sizes from $L = 2^5$ to $L = 2^{13}$ in powers of 2.), the width displays an initially linear growth as in fully wet systems before the effect of the nonlinearity triggers a growth faster than a power law. The saturation time does not seem to depend on system size, at odds with the standard roughening scenario. c) Values of the saturated width as a function of system size corresponding to the unscreened limit in perfect agreement with our analytical prediction that $\chi = 1$ (orange line).

timescale proportional to $1/|\mathbf{q}|^3$ when the bulk dynamics of the mass density is diffusive [2, 16], it is surprising that we find the same relaxation timescale in our case, in which the bulk dynamics is dominated by long-ranged fluid flows. Second, our wet setting allows us to connect the active forces directly to the amplitude of the nonlinearity in the interface equation; this is at odds with systems with diffusive bulk dynamics, in which the $|\mathbf{q}|$ KPZ nonlinearity only arises as an effect of fluctuations along the RG flow [19].

To confirm our prediction that the interface belongs to the $|\mathbf{q}|$ KPZ universality class in the presence of friction, we integrated Eq. (12) numerically for strong friction. The evolution of the interface width W^2 with time is reported in Fig. 2a) for $\lambda = 10^3$: While in the linear case, we observe a mean-field growth $W^2 \sim t^{1/3}$ [44], for sufficiently large systems ($L \gtrsim 256$) and late times the growth is consistent with $2\chi/z \approx 0.28$, the value predicted for the $|\mathbf{q}|$ KPZ universality class.

Having described the ultimate large-scale behaviour of Eq. (12), we now rationalise the early-time regime. To do so, we consider the regime $\lambda \rightarrow 0$ while retaining a finite α , which we refer to as the unscreened limit in the following. From Eq. (11), we obtain that

$$\mathcal{T}_{yy}(\mathbf{q}, 0) \rightarrow_{\lambda \rightarrow 0} \frac{1}{4\eta|\mathbf{q}|}, \quad (16)$$

and hence (12) becomes

$$\partial_t h_{\mathbf{q}}(t) = -\frac{\gamma|\mathbf{q}|}{4\eta} h_{\mathbf{q}}(t) + \frac{\alpha}{4\eta|\mathbf{q}|} \mathcal{F}[(\nabla h(\mathbf{x}, t))^2] + \xi_{\mathbf{q}}. \quad (17)$$

The linear roughening properties of Eq. (17) can be read

off by setting $\alpha = 0$, which gives $z = 1$ and $2\chi = 2 - d$. To go beyond the linear regime, we perform a standard one-loop RG analysis [10]. Interestingly, all one-loop diagrams vanish with the exception of the noise renormalization [44], which generates a noise with a lower order correlation than the one in Eq. (17). That is, the nonlinearity α generates $\xi_{\mathbf{q}}'(t)$ which has zero average and correlations

$$\langle \xi_{\mathbf{q}}'(t) \xi_{\mathbf{q}'}'(t') \rangle = \frac{D'}{|\mathbf{q}|^2} (2\pi)^d \delta(\mathbf{q} + \mathbf{q}') \delta(t - t'), \quad (18)$$

where D' is a function of the dimensionless nonlinearity $\bar{\alpha}$ and of the ultraviolet cut-off Λ , see [44] for the explicit expression.

Eq. (18) implies a static structure factor $S(\mathbf{q}) \sim |\mathbf{q}|^{-3}$, and $\chi = (3 - d)/2$. When $d = 1$, this implies $\chi = 1$, which is believed on general grounds to be the upper bound for the roughness exponent associated with interfaces without overhangs [10]. Furthermore, the correlator $\langle |\delta \mathbf{n}(\mathbf{x}) - \delta \mathbf{n}(\mathbf{0})|^2 \rangle$ for fluctuations of the normal $\delta \mathbf{n} \approx \nabla h$ now diverges logarithmically with distance, i.e. the interface becomes random beyond a de Gennes-Taupin lengthscale $\propto e^{\gamma/D'}$. Correspondingly, the normal, averaged over space, vanishes, $\lim_{L \rightarrow \infty} (1/L) \int d\mathbf{x} \delta \mathbf{n} = 0$. Interestingly, while the original de Gennes-Taupin lengthscale was obtained for a tension-free membrane and depends on the bending rigidity [46], here it depends on the surface tension. We finally observe that $\chi = 1$ in $d = 1$ means that the scaling dimension of ∇h vanishes, implying that any power of ∇h becomes equally relevant in the RG sense.

To verify our predictions for the early time dynamics

of the interfaces, we studied Eq. (17) numerically in the unscreened limit. Fig. 2b reports the time evolution of the interfacial width. At early times, $W^2 \sim t$, which corresponds to the linear behaviour of Eq. (12), before that the non-linearity induces a faster growth which does not seem to be described by a power law. This is compatible with what was already observed by numerically integrating the full interface equation (12), see Fig. 1, confirming that the unscreened limit describes the early-time dynamics of the interface. Furthermore, the scaling of the saturated width with L fits a power law $W^2 \sim L^{1.99}$, extremely close to the prediction previously obtained analytically ($\chi = 1$, corresponding to $W_\infty^2 \sim L^2$). Interestingly, the timescale at which W^2 saturates is found to be system-size independent, a fact that is not explained by the standard roughening scenario.

We finally consider the regime in which the system is fully wet. In this case, in addition to λ being 0, all force densities entering the Stokes equation arise from the divergence of a stress tensor. This rules out the active force in Eq. (6) except when $K_1 - 2K_2 = 0$ (in which case the associated stress tensor is $\sigma_{ij}^a = \phi(\nabla_i \phi \nabla_j \phi - \delta_{ij}(\nabla \phi)^2/2)$). More generally, we consider the most general stress tensor to order $\mathcal{O}(\nabla^2)$ and any order in the density: $\sigma_{ij} = -\kappa(\phi)\partial_i \phi \partial_j \phi$, with $\kappa(\phi)$ being an arbitrary function of ϕ . This includes Active Model H as a special case when κ is constant and the active forces in Eq. (6) when $K_1 - 2K_2 = 0$. Following the same steps as those for obtaining Eq. (12), we show that $\alpha = 0$ in this case [44]: with full momentum conservation, we only find non-linearities that are irrelevant from an RG point of view. Therefore, although we cannot exclude that a relevant non-linearity is produced by even more general forms of σ_{ij} , or by fluctuations along the RG flow once irrelevant non-linearities are included, our results suggest that the interface equation in the fully wet limit is linear even in an active setting; we thus expect that this case is fully described by eq. (1) with $a = 1$.

In conclusion, we have described interfaces in wet phase-separated active systems. In the presence of fluid friction, we have shown that they belong, at sufficiently large scales, to the $|\mathbf{q}|$ KPZ universality class. This result is surprising because the fluid flow, although screened, induces long-range interactions that are non-diffusive. We have further shown that the early-time dynamics of these interfaces are analogous to those in momentum-conserved systems. The two regimes are connected by a fast growth that is not described by the standard roughening scenario but can be rationalised by neglecting the friction between the substrate and the fluid; in this regime, the static structure factor is not described by the standard capillary-wave theory.

It would be interesting to investigate the relevance of our work for confluent biological tissues: although we expect the same fundamental physics as the one described here, interfaces are significantly sharper than in

fluids [47, 48]. Our results may also prove relevant for recent experiments on phase-separated active fluids, which are currently able to probe scales at which the system is isotropic on average [26, 49]. Techniques similar to those employed here may be used to describe shape fluctuations of biomolecular condensates [50, 51], in which the effect of fluid flow has only recently been investigated [52, 53].

FC thanks Cristina Marchetti, Paarth Gulati and Aparna Baskaran for useful discussions. FC acknowledges support from the NSF, grants DMR-2041459 & DMR-2011846. AM and CN acknowledge the support of the ANR grant PSAM. CN acknowledges the support of the INP-IRP grant IFAM and from the Simons Foundation. AM and CN thank the Isaac Newton Institute for Mathematical Sciences for the support and hospitality during the program ‘‘Anti-diffusive dynamics: from sub-cellular to astrophysical scales’’ when part of this work was undertaken.

* fcaballero@brandeis.edu

- [1] J. Krug, Origins of scale invariance in growth processes, *Adv. Phys.* **46**, 139 (1997).
- [2] A. J. Bray, Theory of phase-ordering kinetics, *Adv. Phys.* **43**, 357 (1994).
- [3] H. Peters, D. Stauffer, H. Hölters, and K. Loewenich, Radius, perimeter, and density profile for percolation clusters and lattice animals, *Z. Phys. B Con. Mat.* **34**, 399 (1979).
- [4] M. Plischke and Z. Rácz, Active zone of growing clusters: Diffusion-limited aggregation and the eden model, *Phys. Rev. Lett.* **53**, 415 (1984).
- [5] R. Jullien and R. Botet, Scaling properties of the surface of the eden model in $d = 2, 3, 4$, *J. Phys. A-Math. Gen.* **18**, 2279 (1985).
- [6] M. Eden, A probabilistic model for morphogenesis, in *Symposium on information theory in biology* (Pergamon Press, New York, 1958) pp. 359–370.
- [7] F. Family and T. Vicsek, Scaling of the active zone in the eden process on percolation networks and the ballistic deposition model, *J. Phys. A-Math. Gen.* **18**, L75 (1985).
- [8] D. Forster, D. R. Nelson, and M. J. Stephen, Large-distance and long-time properties of a randomly stirred fluid, *Phys. Rev. A* **16**, 732 (1977).
- [9] M. Kardar, G. Parisi, and Y.-C. Zhang, Dynamic scaling of growing interfaces, *Phys. Rev. Lett.* **56**, 889 (1986).
- [10] U. C. Täuber, *Critical dynamics: a field theory approach to equilibrium and non-equilibrium scaling behavior* (Cambridge University Press, 2014).
- [11] T. Sun, H. Guo, and M. Grant, Dynamics of driven interfaces with a conservation law, *Phys. Rev. A* **40**, 6763 (1989).
- [12] F. Caballero, C. Nardini, F. van Wijland, and M. E. Cates, Strong coupling in conserved surface roughening: a new universality class?, *Phys. Rev. Lett.* **121**, 020601 (2018).
- [13] A. J. Bray, A. Cavagna, and R. D. Travasso, Interface fluctuations, burgers equations, and coarsening under shear, *Phys. Rev. E* **65**, 016104 (2001).

- [14] A. Shinozaki, Dispersion relation around a kink solution in binary fluids undergoing spinodal decomposition, *Phys. Rev. E* **48**, 1984 (1993).
- [15] J. S. Rowlinson and B. Widom, *Molecular theory of capillarity* (Courier Corporation, 2013).
- [16] G. Fausti, E. Tjhung, M. Cates, and C. Nardini, Capillary interfacial tension in active phase separation, *Phys. Rev. Lett.* **127**, 068001 (2021).
- [17] F. Caballero and M. C. Marchetti, Activity-suppressed phase separation, *Phys. Rev. Lett.* **129**, 268002 (2022).
- [18] P. Gulati, F. Caballero, I. Kolvin, Z. You, and M. C. Marchetti, Traveling waves at the surface of active liquid crystals, arXiv preprint arXiv:2407.04196 (2024).
- [19] M. Besse, G. Fausti, M. E. Cates, B. Delamotte, and C. Nardini, Interface roughening in nonequilibrium phase-separated systems, *Phys. Rev. Lett.* **130**, 187102 (2023).
- [20] M. C. Marchetti, J.-F. Joanny, S. Ramaswamy, T. B. Liverpool, J. Prost, M. Rao, and R. A. Simha, Hydrodynamics of soft active matter, *Rev. Mod. Phys.* **85**, 1143 (2013).
- [21] F. Jülicher, S. W. Grill, and G. Salbreux, Hydrodynamic theory of active matter, *Rep. Prog. Phys.* **81**, 076601 (2018).
- [22] J. Palacci, S. Sacanna, A. P. Steinberg, D. J. Pine, and P. M. Chaikin, Living crystals of light-activated colloidal surfers, *Science* **339**, 936 (2013).
- [23] T. Sanchez, D. T. Chen, S. J. DeCamp, M. Heymann, and Z. Dogic, Spontaneous motion in hierarchically assembled active matter, *Nature* **491**, 431 (2012).
- [24] A. Bricard, J.-B. Caussin, N. Desreumaux, O. Dauchot, and D. Bartolo, Emergence of macroscopic directed motion in populations of motile colloids, *Nature* **503**, 95 (2013).
- [25] A. E. Patteson, A. Gopinath, and P. E. Arratia, The propagation of active-passive interfaces in bacterial swarms, *Nat. Comm.* **9**, 5373 (2018).
- [26] R. Adkins, I. Kolvin, Z. You, S. Witthaus, M. C. Marchetti, and Z. Dogic, Dynamics of active liquid interfaces, *Science* **377**, 768 (2022).
- [27] A. M. Tayar, F. Caballero, T. Anderberg, O. A. Saleh, M. Cristina Marchetti, and Z. Dogic, Controlling liquid-liquid phase behaviour with an active fluid, *Nat. Mater.* **22**, 1401 (2023).
- [28] P. Galajda, J. Keymer, P. Chaikin, and R. Austin, A wall of funnels concentrates swimming bacteria, *J. Bact.* **189**, 8704 (2007).
- [29] H. Diamant, Hydrodynamic interaction in confined geometries, *J. Phys. Soc. Jpn* **78**, 041002 (2009).
- [30] A. Maitra, P. Srivastava, M. C. Marchetti, S. Ramaswamy, and M. Lenz, Swimmer suspensions on substrates: anomalous stability and long-range order, *Phys. Rev. Lett.* **124**, 028002 (2020).
- [31] L. Chen, C. F. Lee, and J. Toner, Mapping two-dimensional polar active fluids to two-dimensional soap and one-dimensional sandblasting, *Nat. Comm.* **7**, 12215 (2016).
- [32] A. Bricard, J.-B. Caussin, N. Desreumaux, O. Dauchot, and D. Bartolo, Emergence of macroscopic directed motion in populations of motile colloids, *Nature* **503**, 95 (2013).
- [33] T. Brotto, J.-B. Caussin, E. Lauga, and D. Bartolo, Hydrodynamics of confined active fluids, *Phys. Rev. Lett.* **110**, 038101 (2013).
- [34] N. Sarkar, A. Basu, and J. Toner, Swarming bottom feeders: flocking at solid-liquid interfaces, *Phys. Rev. Lett.* **127**, 268004 (2021).
- [35] M. E. Cates and E. Tjhung, Theories of binary fluid mixtures: from phase-separation kinetics to active emulsions, *J. Fluid Mech.* **836**, P1 (2018).
- [36] P. C. Hohenberg and B. I. Halperin, Theory of dynamic critical phenomena, *Rev. Mod. Phys.* **49**, 435 (1977).
- [37] A. Oron, S. H. Davis, and S. G. Bankoff, Long-scale evolution of thin liquid films, *Rev. Mod. Phys.* **69**, 931 (1997).
- [38] A. Maitra, P. Srivastava, M. C. Marchetti, J. S. Lintuvuori, S. Ramaswamy, and M. Lenz, A nonequilibrium force can stabilize 2d active nematics, *Proc. Nat. A. Sci.* **115**, 6934 (2018).
- [39] A. Tiribocchi, R. Wittkowski, D. Marenduzzo, and M. E. Cates, Active model h: scalar active matter in a momentum-conserving fluid, *Phys. Rev. Lett.* **115**, 188302 (2015).
- [40] J. Prost and R. Bruinsma, Shape fluctuations of active membranes, *Europhysics Letters* **33**, 321 (1996).
- [41] F. Cagnetta, V. Škultéty, M. R. Evans, and D. Marenduzzo, Universal properties of active membranes, *Physical Review E* **105**, L012604 (2022).
- [42] S. Ramaswamy, J. Toner, and J. Prost, Nonequilibrium fluctuations, traveling waves, and instabilities in active membranes, *Physical review letters* **84**, 3494 (2000).
- [43] Notice that it has a non-zero value in the steady state $2\alpha\delta(y)\hat{y}$. It can be shown that this leads only to a pressure jump at the interface and not to a steady motion.
- [44] See Supplemental Material at [URL will be inserted by publisher] which presents additional numerical results and details.
- [45] F. Caballero, cuPSS: a package for pseudo-spectral integration of stochastic PDEs, arXiv preprint arXiv:2405.02410 (2024).
- [46] P. De Gennes and C. Taupin, Microemulsions and the flexibility of oil/water interfaces, *J. Phys. Chem.* **86**, 2294 (1982).
- [47] D. M. Sussman, J. Schwarz, M. C. Marchetti, and M. L. Manning, Soft yet sharp interfaces in a vertex model of confluent tissue, *Phys. Rev. Lett.* **120**, 058001 (2018).
- [48] H. Yue, C. R. Packard, and D. M. Sussman, Scale-dependent sharpening of interfacial fluctuations in shape-based models of dense cellular sheets, arXiv preprint arXiv:2407.02760 (2024).
- [49] L. Zhao, P. Gulati, F. Caballero, I. Kolvin, R. Adkins, M. C. Marchetti, and Z. Dogic, Asymmetric fluctuations and self-folding of active interfaces, arXiv preprint arXiv:2407.04679 (2024).
- [50] J. O. Law, C. M. Jones, T. Stevenson, T. A. Williamson, M. S. Turner, H. Kusumaatmaja, and S. N. Grellscheid, A bending rigidity parameter for stress granule condensates, *Science Advances* **9**, eadg0432 (2023).
- [51] C. M. Caragine, S. C. Haley, and A. Zidovska, Surface fluctuations and coalescence of nucleolar droplets in the human cell nucleus, *Physical review letters* **121**, 148101 (2018).
- [52] R. Seyboldt and F. Jülicher, Role of hydrodynamic flows in chemically driven droplet division, *New journal of physics* **20**, 105010 (2018).
- [53] N. Galvanetto, M. T. Ivanović, A. Chowdhury, A. Sottini, M. F. Nüesch, D. Nettel, R. B. Best, and B. Schuler, Extreme dynamics in a biomolecular condensate, *Nature*

619, 876 (2023).

Supplementary Information: Interface dynamics of wet active systems

Fernando Caballero,¹ Ananyo Maitra,^{2,3} and Cesare Nardini^{4,5}

¹*Department of Physics, Brandeis University, Waltham, MA 02453, USA**

²*Laboratoire de Physique Théorique et Modélisation, CNRS UMR 8089, CY Cergy Paris Université, F-95032 Cergy-Pontoise Cedex, France*

³*Laboratoire Jean Perrin, UMR 8237 CNRS, Sorbonne Université, 75005 Paris, France*

⁴*Service de Physique de l'Etat Condensé, CEA, CNRS Université Paris-Saclay, CEA-Saclay, 91191 Gif-sur-Yvette, France*

⁵*Sorbonne Université, CNRS, Laboratoire de Physique Théorique de la Matière Condensée, LPTMC, F-75005 Paris, France*
(Dated: September 12, 2024)

I. NUMERICAL DETAILS

The numerics shown in the main text have all been done using a pseudo-spectral scheme, using both in-house developed Python code, and cuPSS [1]. The particular solvers over the cuPSS library are available upon request.

Every curve in Fig. 1 and Fig. 2 of the main texts, as well as Figs 1 and 2 of this SM are obtained averaging over between 10^2 and 10^3 different noise realizations, depending on the system-size. In all runs we have set $\gamma = 1$ and $D = 0.01$ while other parameters have been defined in the text. The results have been presented in terms of the non-dimensional coupling constant $\bar{\alpha} = \alpha D^{1/2} \gamma^{-3/2}$ so that $\alpha = 10\bar{\alpha}$.

Fig. 1(Left) report numerical simulations of Eq. (11) in the main text for $\lambda = 0$ and $\alpha = 0$, for which we expect linear growth W^2 at early times, and the saturated value W_∞^2 to be linearly increasing with system size. This is indeed what we observe in Fig. 1(Left). Fig. 1(Right) instead shows numerics of Eq. (11) with $\lambda = 10^3$ and $\alpha = 0$. As expected, we now observe $W^2 \sim t^{1/3}$.

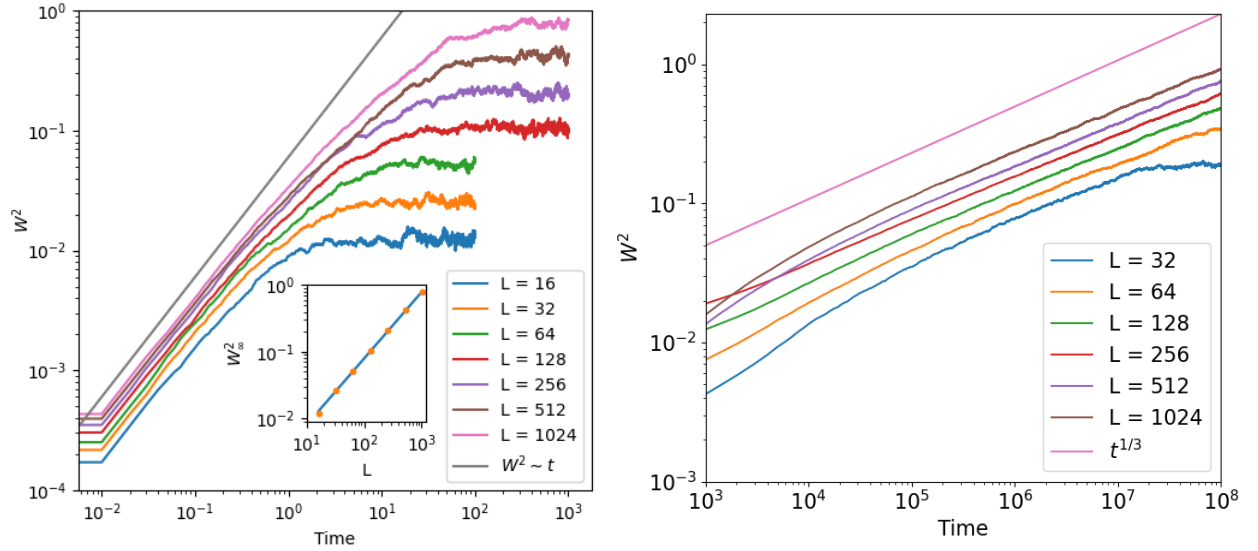


FIG. 1. Simulations of Eq. (11) in the linear case $\alpha = 0$ showing that we obtain the expected scaling. (Left) $\lambda = 0$, we report the growth of the interface width W^2 in time and (inset) the saturated value W_∞^2 as a function of system-size. These are in perfect agreement with the predicted scaling $2\chi = 1$ and $z = 1$. The line in the inset has slope 1.00. (Right) For $\lambda = 10^3$, we obtain $z = 1/3$ again in perfect agreement with the expected mean-field results.

* fcaballero@brandeis.edu

II. DERIVATION OF EQ. (11) FOR NORMAL ACTIVE FORCES

This section shows the derivation of Eq. (11) of the main text, using the force \mathbf{f}^a in Eq. (6) of the main text. Expanding this force to quadratic order in ∇h , we obtain that $\mathbf{f}^a = 2\alpha_f(\hat{y} - \hat{x}\nabla h - \frac{1}{2}\hat{y}(\nabla h)^2)\delta(y - h(\mathbf{x}))$. Notice the first two terms amount to a pressure term proportional to ϕ and thus can be ignored in the calculation of the flow. We thus have that $\mathbf{f}^a = -\alpha_f\hat{y}(\nabla h)^2\delta(y - h(\mathbf{x})) + O(h^3)$. Additionally, there is an equilibrium capillary force $\mathbf{f}^p = -\phi\nabla\mu$, that generates a single non vanishing force responsible for interface tension [2].

Writing Eq. (7) of the main text for both the equilibrium and nonequilibrium forces, we obtain

$$-\varphi'(u)\partial_t h(\mathbf{x}, t) = -\varphi'(u) \int d\mathbf{x}' dy' T_{ij}(\mathbf{x} - \mathbf{x}', h(\mathbf{x}, t) - h(\mathbf{x}', t)) (f_j^p(\mathbf{x}', y') + f_j^a(\mathbf{x}', t)), \quad (1)$$

where we have defined $u = y - h(\mathbf{x}, t)$. We can now substitute the values of the two forces to lowest order in $h(\mathbf{x}, t)$. To do so, notice the first term in the force, which is the equilibrium capillary force, is responsible for the linear interfacial tension term, the only term that remains in equilibrium. Notice as well that that, as explained in the paragraph above, \mathbf{f}^a is already quadratic in ∇h to lowest order. With this in mind, we can write

$$-\varphi'(u)\partial_t h(\mathbf{x}, t) = -\gamma\varphi'(u) \int d\mathbf{x}' T_{yy}(\mathbf{x} - \mathbf{x}', 0)\nabla^2 h(\mathbf{x}', t) + \alpha_f\varphi'(u) \int d\mathbf{r}' T_{yy}(\mathbf{r} - \mathbf{r}')(\nabla h(\mathbf{x}', t))^2 + O(h^3), \quad (2)$$

Again, the first term is the equilibrium term, while the second is the only non vanishing term to quadratic order. We now multiply the equation with $\varphi'(u)$ and integrate across the interface to obtain

$$\partial_t h(\mathbf{x}, t) = \gamma \int d\mathbf{x}' T_{yy}(\mathbf{x} - \mathbf{x}', 0)\nabla^2 h(\mathbf{x}', t) - \alpha_f \int d\mathbf{x}' dy' T_{yy}(\mathbf{x} - \mathbf{x}', h(\mathbf{x}, t) - h(\mathbf{x}', t))(\nabla h(\mathbf{x}', t))^2 + O(h^3). \quad (3)$$

We can then expand T_{yy} in h in the second term of the r.h.s. and keep only the zeroth order term, since this already generates the lowest order term quadratic in h . We obtain

$$\partial_t h(\mathbf{x}, t) = \gamma \int d\mathbf{x}' T_{yy}(\mathbf{x} - \mathbf{x}', 0)\nabla^2 h(\mathbf{x}', t) - \alpha_f \int d\mathbf{x}' dy' T_{yy}(\mathbf{x} - \mathbf{x}', 0)(\nabla h(\mathbf{x}', t))^2. \quad (4)$$

which is Eq. (11) of the main text written in real space.

III. QUADRATIC NONLINEARITIES ARE NOT GENERATED BY A STRESS

This section shows that including the nonequilibrium stress

$$\sigma_{ij} = -k\partial_i\phi\partial_j\phi - \kappa(\phi)\partial_i\phi\partial_j\phi, \quad (5)$$

does not generate quadratic nonlinearities for any local function $\kappa(\phi)$, as long as the sharp-interface limit is considered. Notice the equilibrium stress is recovered for $\kappa(\phi) = 0$ and Active Model H when $\kappa(\phi)$ is constant.

Consider the equation for $h(\mathbf{x}, t)$, as derived from the ansatz $\phi = \varphi(y - h(\mathbf{x}, t))$, obtained from Eq. (7) of the main text, multiplying it with $\varphi'(u)$ and integrating across the interface:

$$\partial_t h = - \int d\mathbf{x}' dy' T_{yy}(\mathbf{x} - \mathbf{x}', h(\mathbf{x}) - y')\partial_k\sigma_{yk} + \nabla h \int d\mathbf{x}' dy' T_{xx}(\mathbf{x} - \mathbf{x}', h(\mathbf{x}) - y')\partial_k\sigma_{xk}. \quad (6)$$

The sharp interface limit further allows us to write the stress as located at the interface, and thus we can further write

$$\partial_t h = - \int d\mathbf{x}' T_{yy}(\mathbf{x} - \mathbf{x}', h(\mathbf{x}) - h(\mathbf{x}')) \int_{-\infty}^{\infty} dy' \partial_k\sigma_{yk} + \nabla h \int d\mathbf{x}' T_{xx}(\mathbf{x} - \mathbf{x}', h(\mathbf{x}) - h(\mathbf{x}')) \int_{-\infty}^{\infty} dy' \partial_k\sigma_{xk}. \quad (7)$$

Observe that the integrals over y' contain terms of the form $\partial_k\sigma_{ij}$, and thus are total derivatives; they vanish when $k = y$ because the stress at infinity does vanish. We further expand each T_{ij} in the height fields, keeping only the lowest order (see Eq. (10) of the main text). We are thus left with

$$\partial_t h = - \int d\mathbf{x}' T_{yy}(\mathbf{x} - \mathbf{x}', 0) \int_{-\infty}^{\infty} dy' \nabla\sigma_{yx} + \nabla h \int d\mathbf{x}' T_{xx}(\mathbf{x} - \mathbf{x}', 0) \int_{-\infty}^{\infty} dy' \nabla\sigma_{xx}. \quad (8)$$

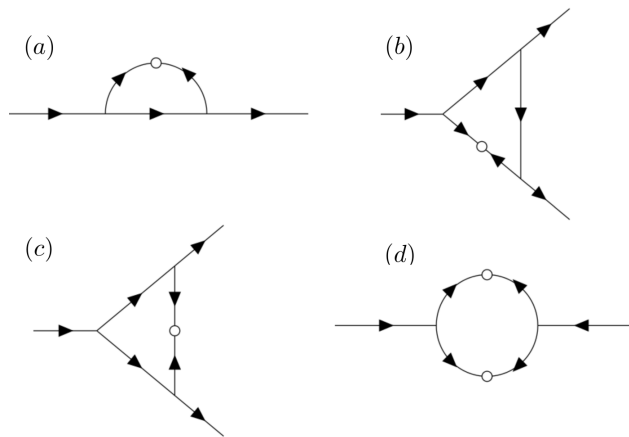


FIG. 2. One loop Feynman diagrams for an equation with quadratic vertex functions.

It can be shown that σ_{xx} is of order $(\nabla h)^2$, and thus the second term in the r.h.s. does not contain quadratic terms. Expanding the derivative in the first term of the r.h.s., we obtain

$$\nabla \sigma_{xy} = [k + \kappa(\varphi(u'))]\varphi'(u')^2 \nabla^2 h + k \partial_{u'}[\varphi'(u')^2](\nabla h)^2 + \partial_{u'}[f(\varphi(u'))\varphi'(u')^2](\nabla h)^2. \quad (9)$$

The first term in the r.h.s. is diffusion, albeit with a renormalized by κ . The second and third terms are total derivatives in y' , and will thus give no contribution when integrated over y' . Hence, the interface equation reduces to the linear equation (1) of the main text where we have omitted nonlinearities that are higher order than quadratic in h . Our result thus shows that, when the stress tensor is as in Eq. (5), quadratic nonlinearities do not arise in the interface equation, at least at bare level.

IV. DERIVATION OF EQ. (11) FOR ACTIVE FORCES FROM THE GRADIENT EXPANSION

This section shows that a force of the form of Eq. (5) in the main text produces a term of the same form as the nonlinearity of Eq. (11). We show it here for the y component of the force. Expanding Eq. (5) of the main text using $\phi(\mathbf{x}, y, t) = \varphi(y - h(\mathbf{x}, t))$, we obtain

$$\begin{aligned} f_y^a &= K_1 \phi(\nabla^2 \phi) \partial_y \phi + K_2 |\nabla \phi|^2 \partial_y \phi \\ &= (K_1 \varphi(u) \varphi'(u) \varphi''(u) + K_2 \varphi'(u)^3)(1 + (\nabla h)^2). \end{aligned} \quad (10)$$

The terms that do not depend on h account for pressure jumps across the interface, and can thus be ignored. To proceed, we note that $\partial_u(\varphi(u)\varphi'(u)^2) = \varphi'(u)^3 + 2\varphi(u)\varphi'(u)\varphi''(u)$. Using this equality, we can rewrite the previous equation as

$$f_y^a = K_2 \partial_u(\varphi(u)\varphi'(u)^2)(\nabla h)^2 + (K_1 - 2K_2)\varphi(u)\varphi'(u)\varphi''(u)(\nabla h)^2. \quad (11)$$

The first term is a total derivative and will thus vanish when integrating across the interface, as shown in the previous section, when substituting this force in Eq. (6). The second term is the same nonlinearity as in Eq. (11), when setting, as described there, $\alpha = (K_1 - 2K_2)\varphi(u)\varphi'(u)\varphi''(u)$. In the particular case $K_1 - 2K_2 = 0$, we can write the force in Eq. (5) of the main text as the divergence of a stress $\sigma_{ij} \sim \phi(\nabla_i \phi \nabla_j \phi - \delta_{ij}(\nabla \phi)^2/2)$, equivalent to including higher order terms in the stiffness κ in the free energy, i.e. $\kappa \rightarrow \kappa + \kappa' \phi$. This is compatible with the result of Appendix III.

V. RENORMALIZATION DIAGRAM CALCULATIONS

We consider here the one-loop Feynman diagrams for Eq. (16) of the main text, and show that a new noise with variance as in Eq. (17) in the main text is generated. We use the following notation for the vertex

$$v(\mathbf{q}_1, \mathbf{q}_2, \mathbf{q}_3) = \frac{\alpha}{|\mathbf{q}_1|} \mathbf{q}_2 \cdot \mathbf{q}_3, \quad (12)$$

for the linear propagator $G_0(\mathbf{q}, \omega)$ and correlator $C_0(\mathbf{q}, \omega)$:

$$G_0(\mathbf{q}, \omega) = \frac{1}{-i\omega + \gamma|\mathbf{q}|} \quad ; \quad C_0(\mathbf{q}, \omega) = \frac{2D}{|\mathbf{q}|(\omega^2 + \gamma^2\mathbf{q}^2)}. \quad (13)$$

The following time frequency integrals are also useful

$$\frac{1}{2\pi} \int_{-\infty}^{\infty} d\omega_I G_0(\mathbf{q} - \mathbf{q}_I, -\omega_I) C_0(\mathbf{q}_I, \omega_I) = \frac{D}{\gamma^2} \frac{1}{|\mathbf{q}_I|^2 (|\mathbf{q}_I| + |\mathbf{q} - \mathbf{q}_I|)} \quad (14)$$

and

$$\frac{1}{2\pi} \int_{-\infty}^{\infty} d\omega_I C_0(\mathbf{q} - \mathbf{q}_I, -\omega_I) C_0(\mathbf{q}_I, \omega_I) = \frac{D^2}{\gamma^3} \frac{1}{|\mathbf{q}_I|^3 |\mathbf{q} - \mathbf{q}_I|^2 + |\mathbf{q}_I|^2 |\mathbf{q} - \mathbf{q}_I|^3}. \quad (15)$$

A. Generation of a lower order noise

This subsection shows the result of the calculation of the Feynman diagram that renormalizes the noise, in Fig 2. All other diagrams vanish to one loop. Calling this diagram D_n , we have

$$D_n = 2 \int_{-\infty}^{\infty} \frac{d\omega_I}{2\pi} \int_{|\mathbf{q}_I| \in (\Lambda/b, \Lambda)} \frac{d^d \mathbf{q}_I}{(2\pi)^d} C_0(\mathbf{q}_I, \omega_I) C_0(\mathbf{q} - \mathbf{q}_I, -\omega_I) v(\mathbf{q}, \mathbf{q}_I, \mathbf{q} - \mathbf{q}_I) v(-\mathbf{q}, -\mathbf{q}_I, -\mathbf{q} + \mathbf{q}_I), \quad (16)$$

where the prefactor is the symmetry factor. Calculating this integral by using Eq. 15, and expanding to lowest order in $|\mathbf{q}|$, we obtain

$$D_n = \frac{2D\bar{\alpha}^2 \Lambda^{d-1}}{|\mathbf{q}|^2} db S_d + O(|\mathbf{q}|^{-1}). \quad (17)$$

where $S_d = \Omega_d/(2\pi)^d$, and Ω_d is the surface of a d -dimensional sphere, and where db represents an infinitesimally thin shell of modes that we are integrating out, $b \rightarrow 1 + db$. Eq. (17) shows that a noise with variance proportional to \mathbf{q}^{-2} is generated, as stated in the main text.

-
- [1] F. Caballero, cuPSS: a package for pseudo-spectral integration of stochastic PDEs, arXiv preprint arXiv:2405.02410 (2024).
 [2] A. J. Bray, A. Cavagna, and R. D. Travasso, Interface fluctuations, burgers equations, and coarsening under shear, Phys. Rev. E **65**, 016104 (2001).